Cell Flow PET Simulations as Ground Truth for Development of PET-based Cell Tracking

N. Marquardt[1], T. Hengsbach[1], M. Mauritz[2], B. Wirth[2], K. P. Schäfers[1]

[1]European Institute for Molecular Imaging, University of Münster, Germany; [2]Institute for Computational and Applied Mathematics, University of Münster, Germany

Contact: n.marquardt@uni-muenster.de

Introduction

PET-based cell tracking using coincidence data to follow the pathways of individual radiolabelled cells is an area of active research [1, 2]. To develop and validate these cell tracking algorithms, we are developing cell flow PET simulations (**CeFloPS**) that most realistically model cell flow in humans in clinical scenarios and generate raw PET listmode data through Monte Carlo simulations using GATE. The location and motion of individual cells are constantly recorded and used as ground-truth data.

Methods

CeFloPS is based on the 3D data of organs and blood vessels from the XCAT phantom [3] (Fig. 1). The simulation of the cell path can be divided into a blood flow part along the vessels and a distribution part within the organs, followed by the Monte-Carlo PET simulation using GATE [4].

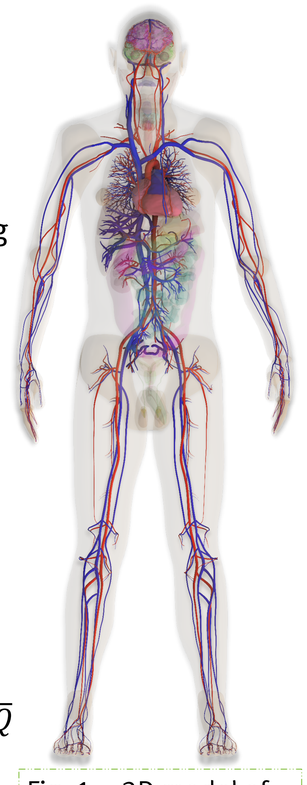

Fig. 1 – 3D model of the XCAT phantom.

Blood flow simulation

- Simplification of XCAT blood vessel system into 1mm-spaced node structure (Fig. 2)
- Calculation of mean blood flow $\bar{Q}$ in each node using Kirchhoff's laws and Hagen-Poiseuille equation:

$$\bar{Q} = \frac{\Delta P}{R}, \qquad R = \frac{8l\eta}{\pi r^4}$$

- Assuming laminar flow, cell velocity profile $v(x)$ is given by

$$v(x) = \frac{2\bar{Q}}{\pi r^2}\left(1 - \frac{x^2}{r^2}\right)$$

- Probabilistic determination of cell path at bifurcations using blood flow distribution:

$$p_i = \frac{Q_{\text{out},i}}{Q_{\text{in}}}, Q_{\text{in}} = \sum_i Q_{\text{out},i}$$

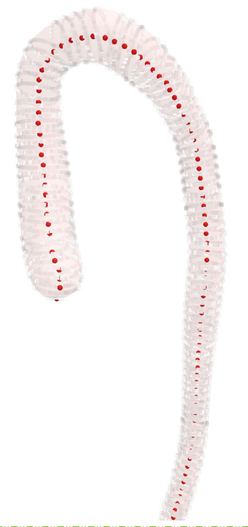

Fig. 2 – Node structure in the aorta.

(ΔP: blood pressure difference, R: vessel resistance, l: vessel length, η: blood viscosity, r: vessel radius, x: radial distance in vessel, p_i: probability for vessel bifurcation i)

Organ distribution simulation

- Organs are voxelized (voxel size 0.125mm^3); voxels with artery entry or vein exit are identified
- Probability vector field in organ is calculated with arteries acting as sources and veins as sinks (Fig. 3)
- Cells perform 3D random walk from artery entry to vein exit, biased by the probability vectors

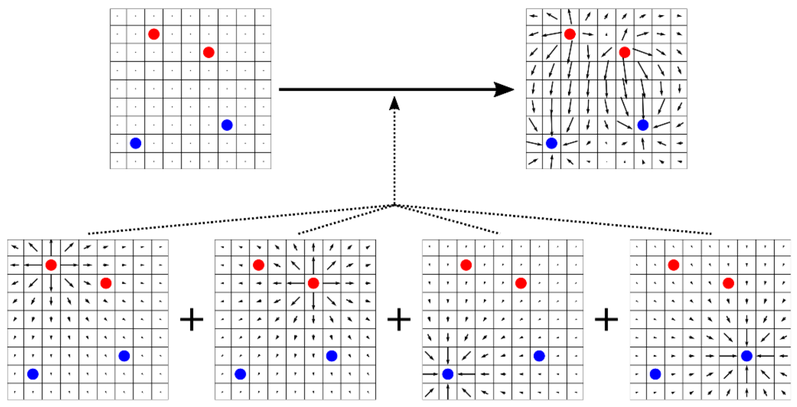

Fig. 3 – 2D representation of the probability vector field used for the random walk inside an organ (red: artery entries, blue: vein exits).

- Cells' speed during random walk is tuned in each organ by physiolocigal references [5]
- Binding in organs in simulated by compartment model (Fig. 4)
- Transitions between compartments are governed by transition matrix G with rate constants k_i
- Probability Π of cell movement or binding is determined using the transition matrix and the length of a time step Δt:

$$\Pi = \exp(\Delta t G)$$

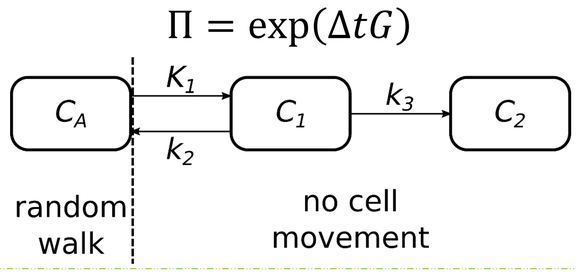

Fig. 4 – Compartment model structure and rate constants for cells physiologically behaving like FDG tracer in an organ. Only cells located in C_A undergo random walk, cells in C_1 are temporarily bound, cells in C_2 permanently.

Monte-Carlo PET simulation

- Spatial coordinates of cells as input for moving radioactive sources (0.1mm spheres) in GATE
- Total-body scanner Biograph Vision Quadra (Siemens Healthineers) implemented as base for simulations
- Attenuation and scatter maps from XCAT phantom
- Simulation of Lutetium-176 background from LSO crystals optional

Results

As an example, the movement of 10 cells with physiological behavior (i.e. transition rates [6]) of FDG tracer and 10kBq each were simulated for 600s in 10ms steps using CeFloPS and GATE (no background). To account for different activities, the generated PET data was reduced to 20%, 5% and 1% of the simulated coincidences. The resulting data was reconstructed using an optimal transport based cell imaging algorithm (**dyn opt**)[7] in comparison to a classical frame-wise expectation maximization method (**fw EM**). To compare both, the time window from 109s to 120s was selected and split into 23 frames (Fig. 5, 6). The difference to the ground truth of both methods was calculated using the Wasserstein-Fisher-Rao metrics described in [8] (Tab. 1).

For animated versions of the results, scan the code to the left!

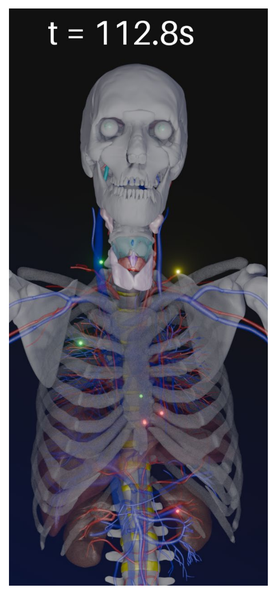

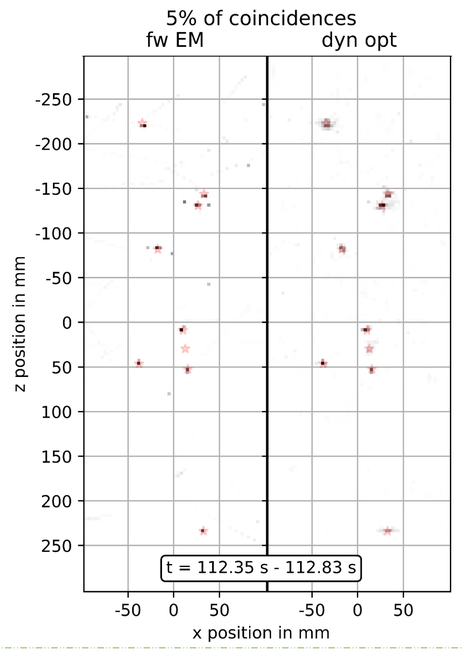

Fig. 5 – Left: Locations of 10 simulated cells in XCAT phantom (red: cells in C_A, yellow: C_1, green: C_2). Right: Reconstructed positions (coronal projection) using fw EM and dyn opt (red stars: ground truth positions).

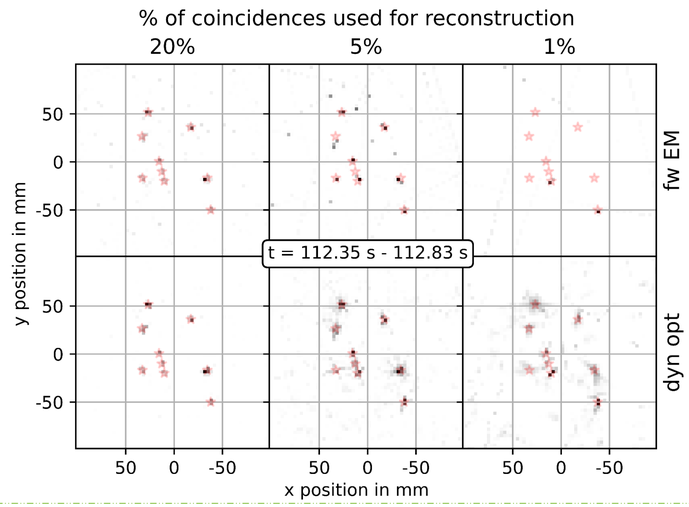

Fig. 6 – Reconstructions (transverse projection) for different numbers of coincidences used.

Tab. 1 – Positional error of fw EM and dyn opt compared to ground truth for different numbers of coincidences and maximal regarded cell transport distance of 29mm.

% of coincidences used	Positional error in mm	
	fw EM	dyn opt
20	18.7	15.5
5	20.2	17.1
1	24.8	18.7

Conclusion

CeFloPS provides a promising approach to simulating cell paths in the human body that closely mimic clinical scenarios. The specific type of cell depends on physiological constraints that govern the motion within organs. PET data generated with CeFloPS and GATE, alongside known ground-truth cell positions, enable quantitative validation and improvement of reconstruction algorithms capable of tracking single or multiple cells using PET.

References

[1] Jung, K. O., et al. (2020). *Nature biomedical engineering*, 4(8): 835-844.

[2] Schmitzer, B., Schäfers, K.P., Wirth, B. (2019). *IEEE Transactions on Medical Imaging*, 39: 1626-1635.

[3] Segars, W.P., Sturgeon, G., Mendonca, S., Grimes, J., Tsui, B.M.W. (2010). *Med. Phys.*, 37: 4902-4915.

[4] Jan, S., Santin, G., Strul, D., et al. (2004). *Phys Med Biol.*, 49(19): 4543-4561.

[5] Leggett, R., Williams, L. (1995). *Health physics*, 69(2): 187-201.

[6] Li, E.J., et al. (2022). *Journal of Nuclear Medicine*, 63(8): 1266-1273.

[7] Mauritz, M., Schmitzer, B., Wirth, B. (2024). *SIAM Journal on Mathematical Analysis*, 56(5): 5840-5880.

[8] Chizat, L., Peyré, G., Schmitzer, B. et al. (2018). *Found Comput Math*, 18: 1–44.

Funded by

Deutsche Forschungsgemeinschaft
German Research Foundation

This work was funded by the Deutsche Forschungsgemeinschaft (DFG) – CRC 1450 – 431460824

inSight CRC 1450